J. Anat. (2006) **208**, pp725–742

Morphological analysis of the hindlimb in apes and humans. II. Moment arms

R. C. Payne,[1] R. H. Crompton,[2] K. Isler,[3] R. Savage,[2] E. E. Vereecke,[4] M. M. Günther,[2] S. K. S. Thorpe[2] and K. D'Août[4]

[1]*Royal Veterinary College, North Mymms, Hatfield, Herts., UK*
[2]*Department of Human Anatomy and Cell Biology, School of Biomedical Sciences, The University of Liverpool, UK*
[3]*Anthropologisches Institut und Museum, Universität Zürich-Irchel, Zürich, Switzerland*
[4]*Department of Biology, Universmity of Antwerp, Belgium*

Abstract

Flexion/extension moment arms were obtained for the major muscles crossing the hip, knee and ankle joints in the orang-utan, gibbon, gorilla (Eastern and Western lowland) and bonobo. Moment arms varied with joint motion and were generally longer in proximal limb muscles than distal limb muscles. The shape of the moment arm curves (i.e. the plots of moment arm against joint angle) differed in different hindlimb muscles and in the same muscle in different subjects (both in the same and in different ape species). Most moment arms increased with increasing joint flexion, a finding which may be understood in the context of the employment of flexed postures by most non-human apes (except orang-utans) during both terrestrial and arboreal locomotion. When compared with humans, non-human great apes tended to have muscles better designed for moving the joints through large ranges. This was particularly true of the pedal digital flexors in orang-utans. In gibbons, the only lesser ape studied here, many of the moment arms measured were relatively short compared with those of great apes. This study was performed on a small sample of apes and thus differences noted here warrant further investigation in larger populations.
Key words force; leg; leverage, locomotion, muscle; primate; tendon.

Introduction

As apes are the closest living relatives of humans, their locomotion is of considerable interest to scientists investigating the evolution of human bipedal gait. In the first part of this study (Payne et al. 2006) we compared the volume and architecture of hindlimb muscles in apes and humans and related the consequences of these features for functional capacity to aspects of locomotor behaviour. However, the functional capacity of a muscle–tendon unit (MTU) is not only governed by the volume and arrangement of the constituent muscle fibres but also by the leverage of that MTU about a joint at different joint angles. Much of the locomotor behaviour of non-human apes involves use of the limbs over a wide range of limb postures. By contrast, human bipedal walking utilizes only a small proportion of the range of mobility of most major lower-limb joints. Thus, variation in MTU moment arms may be expected to have a significant effect on the capacity of each MTU to (1) generate and transfer force and (2) to apply that force at speed, over a wide range of joint positions.

The moment arm of an MTU describes its capacity to rotate a bone about a joint and is defined as the shortest perpendicular distance from the joint centre of rotation (JCR) to the MTU line of action (LOA). Moment arms are capable of influencing the moment-generating capacity of an MTU because a muscle moment (i.e. rotational force) is the product of maximal isometric force and moment arm. Moment arms thus transform muscle force into muscle moments, muscle speed into joint angular speed and muscle excursion into joint excursion (Zajac, 1992). From this, it follows that the amount of joint rotation achieved for a given fibre length change is dependent on a

Correspondence
Dr Rachel Payne, Structure and Motion Laboratory, The Royal Veterinary College, Hawkshead Lane, North Mymms, Hatfield, Hertfordshire AL9 7TA, UK. T: +44 (0)1707 666850; E: rpayne@rvc.ac.uk

Accepted for publication *16 January 2006*

muscle's moment arm. As moment arm increases, the potential for torque production increases at the expense of angular velocity (Lieber & Friden, 2001); thus, muscles with longer fibres are not always associated with joints which have larger ranges of motion, in spite of their ability to work over longer ranges; neither are they necessarily capable of generating high-speed contractions.

Detailed knowledge of muscle geometry is necessary to predict muscle moments and forces accurately. In musculoskeletal modelling, accurate moment arm data permit the transformation of modelled forces into joint moments. By use of models, the forces which are dependent on moment arms can be determined and used to estimate the forces transmitted by the joints during different phases of gait (Brown et al. 2003). Computer-based models are becoming increasingly common in the study of animal locomotion (see, e.g. van den Bogert et al. 1989; Meershoek et al. 2001; Wilson et al. 2001, 2003). Such models are particularly useful in the case of extinct animals (e.g. in birds: Hutchinson, 2002, 2004; in dinosaurs: Carrano & Hutchinson, 2002; Hutchinson & Garcia, 2002) when the only available material is a set of fossil bones. Similarly, computer simulations of locomotion in extinct human relatives have been fruitfully employed to investigate the evolution of human bipedal walking. Simulations where optimized muscle forces are applied to derive motion, that is forwards dynamics simulations (e.g. Sellers et al. 2003, 2004, 2005; Nagano et al. 2005), rather than the pattern of motion being predetermined and used to determine muscle force (inverse-dynamics) (e.g. Crompton et al. 1998) require input data on MTU properties and moment arm trajectories, which data can be obtained from cadaveric dissections of living apes (Li et al. 2002; Wang et al. 2003, 2004; Wang & Crompton, 2004a; 2004b). The only moment arm data that exist for primate hindlimbs to date are those published by Thorpe et al. (1999) and Marzke et al. (1988) for the common chimpanzee. Yet chimpanzees, where locomotion is dominated by terrestrial quadrupedalism (e.g. Pontzer & Wrangham 2004), are rather specialized in terms of their locomotor repertoire and may not represent the best living model for our earliest human ancestors.

There are numerous different methods for measuring muscle moment arms and data exist for a wide range of muscles in humans (Nemeth & Ohlsen, 1985; Spoor & van Leeuwen, 1992; Hughes et al. 1998; Arnold et al. 2000; Juul-Kristensen et al. 2000; Graichen et al. 2001; Maganaris, 2004) and for certain other animals (horses: Meershoek et al. 2001; Brown et al. 2003; frog: Lieber & Boakes, 1988a,b). Moment arms are often determined by physical measurement of the distance between the joint centres of rotation and the line of action of the muscles to be tested (see, e.g. Nemeth & Ohlsen, 1985; Graichen et al. 2001; Meershoek et al. 2001). However, because moment arms have been shown to vary with joint angle (An et al. 1984), methods assuming fixed moment arm values may render estimates of muscle forces inaccurate.

Non-invasive methods such as ultrasound, magnetic resonance imaging and computer tomography are popular methods for measuring aspects of musculoskeletal geometry *in vivo*. Unfortunately, *in vivo* imaging is not practical when studying moment arms in large-bodied apes. The tendon travel method, however, is relatively simple and cost-effective compared with *in vivo* imaging and in terms of procedure does not require knowledge of the position of the JCR, nor does it require separate account to be taken of the geometry of anatomical structures such as the patella. This paper therefore sets out to quantify hindlimb muscle moment arms in extant apes using the tendon travel technique. Variation in the magnitude of moment arm lengths throughout the joint range of motion will be considered in conjunction with aspects of muscle architecture and locomotor behaviour. As with other studies of non-human species, however, the present study of necessity draws from only a small sample of available specimens, and is intended as a contribution to our knowledge of moment arms in a group of scientifically important and yet endangered species. It does not claim to be a definitive survey of moment arm variation within Hominoidea: that awaits further studies which may achieve a more acceptable sample size.

Materials and methods

Subject data

The following cadavers were obtained for this study: one bonobo (*Pan paniscus*), two Western lowland gorilla (*Gorilla gorilla gorilla*), one Eastern lowland gorilla (*Gorilla gorilla graueri*), three orang-utans (*Pongo pygmaeus abelii*) and one gibbon (*Hylobates lar*). Subject data are provided in Table 1. Further detail on the source and post-mortem care of each of the specimens can be found in Payne et al. (2006).

Table 1 Subject data

	Pp	*Gp*	*Gj*	*Gm*	*Oam*	*Ojm*	*Ojf*	*Haf*
Sex	M	M	M	M	M	M	F	F
Age at death (year)	29.6	35	30	33	30	6	5	16
Mass (kg)	64	130	120	120	112	18.7	12.5	4.6
Femur (cm)	28.5	39	35.7	38	29	19	18.6	18.3
Tibia (cm)	27.2	32.5	32.1	43	28	16.8	15.5	15.8
Foot length (cm)	28	32.5	28.7	30.5	27.2	15.6	16.8	10.2

Subjects: *Pp* (*Pan paniscus*), *Gp* (gorilla P), *Gj* (gorilla J), *Gm* (gorilla M), *Oam* (orang-utan adult male), *Ojm* (orang-utan juvenile male), *Ojf* (orang-utan juvenile female), *Haf* (*Hylobates* adult female).

Measurement of muscle moment arms

Flexion/extension moment arms of the major muscles at the hip, knee and ankle were obtained using the tendon-travel method (Landsmeer, 1961; An et al. 1981). The derivative of tendon length with respect to joint angle in revolute joints (which we assume the joints in question to be) is equal to the average perpendicular distance from the JCR to the LOA of the MTU (its moment arm). This is because when a radius of a circle, i.e. the tendon path, moves through an angle of 1 radian, any point on that radius will have moved through an arc equal in length to the radius between that point and the centre of the circle. Thus, the distance that a tendon moves while the limb moves 1 radian equals the average perpendicular distance between the tendon and the joint axis or the moment arm. Hence, muscle moment arms were calculated using the following equation: $MA = dL_m/d\theta$ where MA is the moment arm of the MTU, L_m is the distance moved by the tendon in metres and θ is the joint angle in radians.

To obtain measurements of muscle moment arms, the specimen was arranged on a dissection bench as shown in Fig. 1. Superficial muscles were measured first with the underlying muscles intact, so that muscles remained at their *in vivo* distance from bone.

For all muscles (except fan-shaped muscles, which will be discussed separately below) a length of string with a coloured tag attached was tied around the muscle belly and then fed through a small hook screwed distally into the middle of the point of insertion (to ensure that the string followed the line of action of the MTU). A 20-kN load was applied by a weight hung from the end of the string, to keep the MTU taut. In order to define the axis of the trunk, large plastic map pins were inserted into the greater trochanter and tuber coxae; elsewhere, millimetre scales were attached to the axes of the long bones (medial and lateral: femur, tibia and

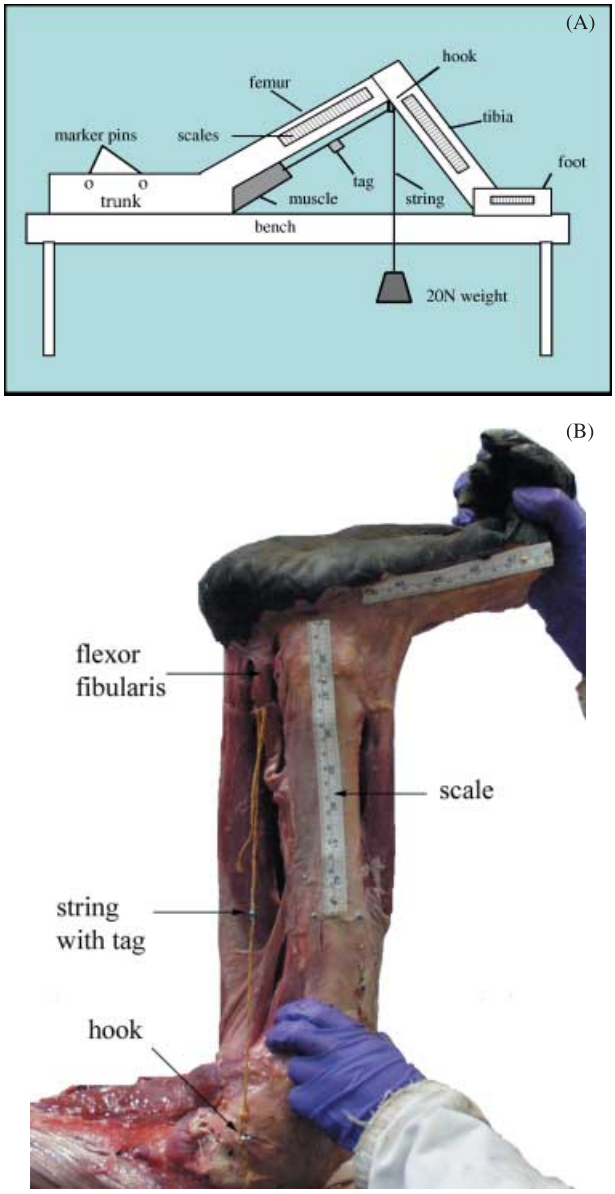

Fig. 1 Experimental set-up for the measurement of muscle moment arms. (A) Diagram showing set-up for biceps femoris at hip. (B) Photograph showing set-up for measuring flexor fibularis at ankle.

fibula; lateral surface of metatarsals I & V). As a joint was flexed and extended, the above-mentioned tag moved along the millimetre scale, allowing measurement of tendon displacement (to the nearest millimetre) and associated joint angle (to the nearest degree) from diapositive or digital images. Images were taken at intervals of approximately 10° from maximum joint extension to maximum joint flexion.

For fan-shaped muscles with wide areas of origin and insertion (i.e. the short head of m. biceps femoris, m. ischiofemoralis, m. gluteus maximus, m. gluteus medius and m. adductor magnus) moment arms were measured by placing a small plastic map pin at the midpoint of both the origin and the insertion of the muscle. The distance between these two pins (the equivalent of tendon displacement) was then measured on the resulting images.

For muscles crossing the hip joint, moment arms were measured by positioning the specimen on its side (freeing motion of the hip joint) and on the floor so that images could be recorded from above the subject, perpendicular to the plane of motion. Slide film data were processed by projecting the image onto a white surface and measuring joint angle and tendon displacement directly from the projected image. For digital images, data were processed using a computer-based image analysis package (Image J, National Institute of Mental Health, Bethesda, MD, USA). The scale nearest to the tendon displacement marker was always used for calibration of length measurements. Tendon displacement was then plotted against joint angle. A linear or second-/third-order polynomial with least-squares fit was used to model this relationship (depending on the line of best fit). Polynomial regression equations were differentiated to give the moment arm value (Hughes et al. 1998). For example, if the line of best fit is linear ($y = mx + c$), the differential of this equation (i.e. the moment arm) is equal to m and will be constant across the range of motion. However, if the line of best fit is described by a polynomial equation (for example: $y = ax^2 - bx + c$) the differential of this equation is $2ax - b$, which gives us the relationship between joint angle and instantaneous moment arm. In the latter case, moment arms change with changing joint angle. Finally, to enable comparison of data between subjects of varying size, moment arm lengths were scaled by either femur length (muscles crossing hip/knee joints) or tibia length (muscles crossing ankle joint).

Results

We were not able to measure all moment arms for all muscles in all subjects. This was either due to measurement error (which could not be detected until after the data were analysed and the muscles had been discarded) or due to damage inflicted during post-mortem examination. Equations for the trend lines fitted to the plots of tendon travel against joint angle are provided in Table 2(A–H). Moment arm curves are provided in Fig. 2. Moment arms were scaled by segment length (see Methods) so that they could be compared between subjects of varying size. Maximum moment arms were determined for each muscle in each subject. The data were then normalized (i.e. divided by femur or tibia length, see Methods) and are provided in Table 3.

Variation in moment arms through joint range of motion

Proximal limb muscle moment arms were generally longer and varied more through joint motion than distal limb muscles. However, the shape and magnitude of moment arm curves varied between subjects, species and between muscle groups. Some moment arm curves showed no change through the joint range of motion, whereas others were linear and increased or decreased with joint flexion; others again were parabolic, moment arms increasing then decreasing or decreasing then increasing with joint flexion. The shape of the moment arm curves was not always the same in members of the same species; for example, the moment arm of m. semitendinosus increased with joint flexion in *Gm* and *Ojm* but remained constant in *Gj* and *Oam*.

Moment arms of muscles crossing the hip joint

The moment arm of m. gluteus maximus at the hip was either parabolic or linear in shape, decreasing then increasing (*Pp* and *Haf*) or just increasing (*Gm*, *Oam*, *Ojm* and *Pt*) with joint flexion. In all subjects, the maximum moment arm occurred in full flexion and was greatest in *Pp*, *Gm* and *Ojm* (19, 24 and 20% of femur length, respectively). In *Pp*, however, it was also at its maximum in full extension. The moment arm of m. gluteus medius at the hip was either parabolic or linear in shape, increasing then decreasing (*Pp*, *Gm* and *Haf*) or just increasing (*Oam* and *Ojm*) with joint

Table 2A Equations of the trend lines fitted to the plots of tendon excursion against joint angle of flexion in *Pp* (*Pan paniscus*)

Muscle tendon unit	Equation	R^2
Gluteus maximus at hip	$y = 1.39x^3 - 6.21x^2 + 9.54x - 0.67$	0.92
Gluteus medius at hip	$y = 0.41x^3 - 1.89x^2 + 1.12x + 2.80$	0.91
Adductor magnus at hip	$y = 1.04x^3 - 6.22x^2 + 5.11x + 10.69$	0.99
Semitendinosus at hip	$y = 0.07x^2 - 4.64x + 10.59$	0.96
Semimembranosus at hip	$y = 0.79x^3 - 4.22x^2 + 0.65x + 10.16$	1.00
Rectus femoris at hip	$y = -0.51x^2 + 4.79x - 1.95$	0.95
Long head of biceps femoris at hip	$y = 0.84x^3 - 4.08x^2 - 0.12x + 12.34$	0.96
Gracilis at hip	$y = 3.81x^2 - 10.33x + 7.46$	0.94
Long head of biceps femoris at knee	$y = -0.49x^2 + 3.01x + 0.11$	0.91
Short head of biceps femoris at knee	$y = -2.70x + 6.58$	0.97
Semitendinosus at knee	$y = 1.03x^2 + 3.62x - 2.04$	0.99
Semimembranosus at knee	$y = 3.17x - 2.18$	0.94
Lateral vastus at knee	$y = -0.73x^2 + 0.18x + 4.41$	0.97
Gracilis at knee	$y = 1.17x^2 + 3.05x - 1.79$	0.98
Lateral gastrocnemius at knee	$y = -0.75x^2 + 3.23x - 0.66$	0.97
Medial gastrocnemius at knee	$y = -0.18x^2 + 1.72x + 0.19$	0.90
Triceps surae at ankle	$y = 0.61x^2 + 1.31x - 3.81$	0.96
Flexor tibialis at ankle	$y = -0.19x^2 - 0.78x + 2.61$	0.98
Flexor fibularis at ankle	$y = 0.07x^2 - 0.85x + 1.97$	0.95
Tibialis anterior at ankle	$y = 2.20x - 1.02$	0.97
Extensor digitorum longus at ankle	$y = 0.02x^2 + 2.98x - 0.94$	1.00
Tibilais posterior at ankle	$y = -0.90x + 2.21$	0.91
Extensor hallucis longus at ankle	$y = 0.28x^2 + 2.37x - 0.68$	0.99

Table 2B Equations of the trend lines fitted to the plots of tendon excursion against joint angle of flexion in *Gp* (*Gorilla gorilla gorilla*)

Muscle tendon unit	Equation	R^2
Long head of biceps femoris at knee	$y = 1.51x - 1.46$	0.99
Short head of biceps femoris at knee	$y = -5.35x + 12.5$	0.95
Semitendinosus at knee	$y = 2.33x^2 + 1.29x - 0.72$	0.98
Semimembranosus at knee	$y = 1.04x^2 + 1.01x + 0.45$	0.98
Lateral vastus at knee	$y = -1.10x^2 - 1.00x + 11.1$	0.97
Gracilis at knee	$y = 1.97x^2 + 1.44x - 0.27$	0.99
Lateral gastrocnemius at knee	$y = 2.49x - 0.94$	0.97
Medial gastrocnemius at knee	$y = 3.19x - 0.41$	0.99
Triceps surae at ankle	$y = 1.48x^2 + 0.66x - 1.41$	0.99
Flexor tibialis at ankle	$y = -0.71x^2 - 2.12x + 7.41$	0.99
Flexor fibularis at ankle	$y = -2.60x + 5.79$	0.95
Tibialis anterior at ankle	$y = -3.65x + 22.0$	0.96
Tibialis posterior at ankle	$y = -1.55x + 3.56$	0.93
Extensor digitorum longus at ankle	$y = 1.86x - 2.05$	0.92
Extensor hallucis longus at ankle	$y = 0.35x^2 + 2.93x - 3.74$	0.99

flexion. Maximum moment arms occurred either in the midrange of joint motion or in full flexion and were relatively large in *Oam* and *Ojm*. The moment arm of m. adductor magnus at the hip was always linear, remaining constant (*Pp*, *Oam*, *Ojm* and *Pt*) with joint flexion at approximately 20–30% of femur length. The moment arm of m. semitendinosus at the hip was always linear, either increasing (*Gm*, *Ojm* and *Haf*) or remaining constant with joint flexion (*Pp*, *Gj*, *Oam* and *Pt*). Maximum moment arms occurred in full flexion. The moment arm of the long head of m. biceps femoris at the hip was either parabolic or linear in shape, increasing then decreasing (*Pp*, *Ojm* and *Haf*), just decreasing (*Gm*) or remaining constant (*Oam* and *Pt*) with joint flexion. Maximum moment arms occurred in the midrange of joint motion or in full extension. The moment arm of m. semimembranosus at the hip was either parabolic or linear in shape, increasing then decreasing (*Pp*), just increasing (*Gm*, *Oam*, *Ojm* and *Haf*) or remaining constant (*Gj* and *Pt*) with joint flexion. Maximum moment arms occurred in the midrange of joint motion or in full flexion. By contrast, the moment arm of m. rectus femoris at the hip was always linear and either decreased (*Pp*, *Oam* and *Ojm*)

Table 2C Equations of the trend lines fitted to the plots of tendon excursion against joint angle of flexion in *Gj* (*Gorilla gorilla gorilla*)

Muscle tendon unit	Equation	R^2
Semitendinosus and semimembranosus at hip	$y = -5.56x + 17.67$	0.87
Rectus femoris at hip	$y = 2.41x - 2.54$	0.90
Long head of biceps femoris at knee	$y = -0.22x^2 + 5.98x + 0.34$	0.99
Short head of biceps femoris at knee	$y = 0.23x^3 - 1.51x^2 + 0.03x + 6.59$	0.98
Lateral vastus at knee	$y = -2.72x + 7.18$	0.99
Semitendinosus at knee	$y = -0.73x^3 + 3.48x^2 + 4.61x - 0.86$	0.98
Semimembranosus at knee	$y = 0.65x^2 + 2.39x + 0.54$	0.99
Gracilis at knee	$y = 0.26x^2 + 3.64x - 0.89$	1.00
Lateral gastrocnemius at knee	$y = -0.72x^2 + 4.61x - 2.70$	0.99
Medial gastrocnemius at knee	$y = -0.19x^2 + 2.03x - 0.21$	0.99
Triceps surae at ankle	$y = -1.83x^2 + 0.83x + 6.66$	0.99
Flexor tibialis at ankle	$y = 1.08x + 2.85$	0.93
Flexor fibularis at ankle	$y = -0.75x^2 + 0.09x - 3.78$	0.98
Tibialis anterior at ankle	$y = 2.30x - 2.01$	0.97
Extensor digitorum longus at ankle	$y = 0.34x^2 + 1.61x + 0.47$	0.90
Extensor hallucis longus at ankle	$y = 0.48x^2 + 2.54x - 1.82$	0.95

Table 2D Equations of the trend lines fitted to the plots of tendon excursion against joint angle of flexion in *Gm* (*Gorilla gorilla graueri*)

Muscle tendon unit	Equation	R^2
Gluteus maximus at hip	$y = -1.98x^2 + 1.15x + 2.32$	0.95
Gluteus medius at hip	$y = 0.84x^3 - 3.51x^2 + 2.72x + 2.27$	0.98
Semitendinosus at hip	$y = 1.52x^2 + 4.07x + 10.2$	0.99
Semimembranosus at hip	$y = 0.76x^2 + 7.77x + 5.19$	0.99
Rectus femoris at hip	$y = -1.82x + 16.6$	0.70
Long head of biceps femoris at hip	$y = -1.30x^2 + 12.4x + 4.99$	0.98
Gracilis at hip	$y = -3.34x^2 + 0.62x + 31.1$	0.98
Long head of biceps femoris at knee	$y = -1.11x + 13.9$	0.91
Lateral vastus at knee	$y = 0.11x^2 + 2.27x + 6.04$	0.83
Lateral gastrocnemius at knee	$y = 0.94x + 23.78$	0.80
Medial gastrocnemius at knee	$y = 1.47x + 7.09$	0.71
Triceps surae at ankle	$y = 0.35x^2 + 4.23x + 10.8$	0.95
Flexor tibialis at ankle	$y = 2.33x + 15.4$	0.98
Flexor fibularis at ankle	$y = 0.45x^2 + 1.52x + 14.6$	0.93
Tibialis anterior at ankle	$y = 4.11x + 33.3$	0.50
Extensor digitorum longus at ankle	$y = -3.20x + 23.3$	0.60

or did not change (*Gj*, *Gm*, *Haf* and *Pt*) with joint flexion. Maximum moment arms occurred at the midrange of joint motion or in full extension. The moment arm of m. gracilis at the hip was always linear, increasing (*Pp*, *Gj*, *Gm* and *Pt*) or remaining constant (*Oam*) with joint flexion. Maximum moment arms occurred in full flexion.

Moment arms of muscles crossing the knee joint

The moment arm of the long head of m. biceps femoris at the knee was always linear, either decreasing (*Pp*, *Gj*, *Oam*, *Haf* and *Pt*) or remaining constant (*Gp*, *Gm*, *Ojm* and *Ojf*) with joint flexion. In *Gm*, it was relatively long through the entire range of joint motion (ranging from 14 to 16% of femur length). Maximum moment arms occurred in full extension. The moment arm of the short head of m. biceps femoris at the knee was similar in magnitude to that of the long head of m. biceps femoris and was either parabolic or linear, increasing then decreasing slightly (*Ojm* and *Gj*), just increasing (*Pt*) or remaining constant (*Pp*, *Gp*, *Gm*, *Oam* and *Haf*) with joint flexion. Maximum moment arms occurred at full flexion. The moment arm of m. semitendinosus at the knee was either parabolic or linear in shape, increasing then decreasing (*Gj* and *Ojf*), just increasing (*Pp*, *Gp*, *Ojm*, *Haf* and *Pt*) or remaining constant (*Oam*) with joint flexion. Maximum moment arms occurred either in the midrange of joint motion or in full extension. The moment arm of m. semimembranosus at the knee was relatively shorter than that of semitendinosus and was always linear, increasing (*Gp*, *Gj*, *Oam* and *Haf*), decreasing (*Ojm* and *Pt*) or remaining constant (*Pp*, *Gm* and *Ojf*) with joint flexion. Maximum

Table 2E Equationms of the trend lines fitted to the plots of tendon excursion against joint angle of flexion in *Oam* (*Pongo pygmaeus abelii*)

Muscle tendon unit	Equation	R^2
Gluteus maximus at hip	$y = -0.27x^3 + 2.21x^2 - 5.12x + 4.05$	0.93
Gluteus medius at hip	$y = 1.04x^2 + 1.52x + 1.66$	0.95
Ischiofemoralis at hip	$y = 2.86x^3 - 9.41x^2 + 4.93x + 4.71$	0.98
Adductor magnus at hip	$y = -7.12x + 13.2$	0.99
Semitendinosus at hip	$y = -8.03x + 15.17$	0.95
Semimembranosus at hip	$y = 0.65x^2 + 6.21x + 8.61$	0.98
Rectus femoris at hip	$y = -0.89x^2 + 6.41x - 3.88$	0.99
Long head of biceps femoris at hip	$y = -7.16x + 11.43$	0.96
Gracilis at hip	$y = 0.27x^2 - 7.80x + 13.6$	0.99
Long head of biceps femoris at knee	$y = -0.12x^2 + 1.97x - 0.88$	0.94
Short head of biceps femoris at knee	$y = -3.27x + 8.31$	0.99
Semitendinosus at knee	$y = 10.3x - 8.5$	0.98
Semimembranosus at knee	$y = 0.75x^2 + 0.65x - 0.76$	0.93
Lateral vastus at knee	$y = -0.19x^2 + 0.03x + 1.17$	0.95
Gracilis at knee	$y = 9.70x - 7.54$	0.98
Lateral gastrocnemius at knee	$y = 0.40x + 0.38$	0.85
Medial gastrocnemius at knee	$y = -0.47^2 + 4.17x - 3.06$	0.89
Triceps surae at ankle	$y = -0.37x^2 - 1.95x + 6.37$	0.96
Flexor tibialis at ankle	$y = 0.48x^2 - 0.42x + 3.62$	0.93
Flexor fibularis at ankle	$y = -0.48x^2 - 0.42x + 3.62$	0.93
Tibialis anterior at ankle	$y = -0.26x^2 + 1.48x - 0.46$	0.96
Extensor hallucis longus at ankle	$y = 0.28x^2 + 2.37x - 0.68$	0.99

Table 2F Equations of the trend lines fitted to the plots of tendon excursion against joint angle of flexion in *Ojm* (*Pongo pygmaeus abelii*)

Muscle tendon unit	Equation	R^2
Gluteus maximus at hip	$y = -0.16x^2 - 0.88x + 2.47$	0.97
Gluteus medius at hip	$y = 0.04x^3 + 0.64x^2 - 0.70x + 0.24$	0.97
Adductor magnus at hip	$y = 4.13x + 3.60$	0.99
Semitendinosus at hip	$y = -0.46x^2 - 1.57x + 5.02$	0.93
Semimembranosus at hip	$y = -0.46x^2 - 1.57x + 5.02$	0.93
Rectus femoris at hip	$y = 0.20x + 2.23$	0.92
Long head of biceps femoris at hip	$y = 0.79x^3 - 3.20x^2 - 0.41x + 7.56$	0.99
Long head of biceps femoris at knee	$y = 1.29x - 0.81$	0.90
Short head of biceps femoris at knee	$y = -0.22x^3 + 1.34x^2 - 0.69x + 0.16$	1.00
Semitendinosus at knee	$y = 0.14x^2 + 4.33x - 0.24$	1.00
Semimembranosus at knee	$y = -0.03x^2 + 1.68x - 0.31$	0.97
Lateral vastus at knee	$y = 0.38x^3 - 1.87x^2 + 0.74x + 4.15$	0.99
Gracilis at knee	$y = 5.82x - 4.93$	1.00
Lateral gastrocnemius at knee	$y = -0.19x^2 + 1.14x + 0.24$	0.99
Medial gastrocnemius at knee	$y = -0.36x^2 + 2.87x - 0.47$	0.99
Triceps surae at ankle	$y = -0.07x^2 - 1.79x + 4.29$	1.00
Flexor tibialis at ankle	$y = -0.97x + 1.99$	0.95
Flexor fibularis at ankle	$y = -1.24x + 3.16$	0.99
Tibialis anterior at ankle	$y = -0.26x^3 + 1.26x^2 - 0.77x + 1.12$	0.99
Tibialis posterior at ankle	$y = 0.09x^2 - 0.74x + 1.39$	0.93
Extensor digitorum longus at ankle	$y = 1.24x + 0.54$	0.97
Extensor hallucis longus at ankle	$y = 0.22x^2 + 1.02x + 0.74$	1.00

moment arms occurred either in the midrange of joint motion, in full flexion or in full extension. The moment arm of m. vastus lateralis at the knee was either parabolic or linear in shape, increasing then decreasing (*Ojm*, *Ojf*, *Haf* and *Pt*), just increasing (*Pp*, *Gp*, *Gm* and *Oam*) or remaining constant (*Gj*) with joint flexion. Maximum moment arms occurred either in the midrange of joint motion or in full flexion. The moment arm of m. gracilis at the knee was always linear, either increasing (*Pp*, *Gp*, *Gj*, *Ojf*, *Haf* and *Pt*) or at a constantly high value (*Oam* and *Ojm*) with joint flexion. Maximum moment arms occurred in full flexion. The moment arm of m. gastrocnemius lateralis at the knee was always linear, either decreasing (*Pp*, *Gj*, *Ojm*, *Ojf* and *Pt*) or remaining constant (*Gp*, *Gm*, *Oam* and *Haf*) with joint flexion. Maximum moment arms

Table 2G Equations of the trend lines fitted to the plots of tendon excursion against joint angle of flexion in *Ojf* (*Pongo pygmaeus*)

Muscle tendon unit	Equation	R^2
Long head of biceps femoris at knee	$y = 1.48x - 0.56$	0.93
Semitendinosus at knee	$y = -0.65x^3 + 2.86x^2 + 0.19x - 0.24$	0.98
Semimembranosus at knee	$y = 1.34x - 0.39$	0.98
Lateral vastus at knee	$y = 0.22x^3 - 1.31x^2 + 1.49x + 1.10$	0.99
Gracilis at knee	$y = 0.66x^2 + 2.68x - 0.86$	0.99
Lateral gastrocnemius at knee	$y = -0.23x^2 + 1.58x - 0.72$	0.99
Medial gastrocnemius at knee (I)	$y = 1.50x - 1.37$	0.99
Medial gastrocnemius at knee (II)	$Y = 2.66x - 1.21$	0.99
Triceps surae at ankle	$y = 0.13x^3 - 0.76x^2 - 0.30x + 4.21$	1.00
Flexor tibialis at ankle	$y = -0.62x + 2.15$	0.96
Flexor fibularis at ankle	$y = 0.14x^3 - 0.65x^2 - 0.01x + 2.50$	0.99
Tibialis anterior at ankle	$y = -0.14x^3 + 0.58x^2 - 0.34x + 0.15$	0.99
Tibialis posterior at ankle	$y = -0.53x + 0.99$	0.89
Extensor digitorum longus at ankle	$y = 1.35x + 0.32$	0.97
Extensor hallucis longus at ankle	$y = -0.10x^2 - 1.90x + 0.65$	0.86

There were two distinct heads (I & II) to gastrocnemius medialis in *Ojm* (see Results for details).

Table 2H Equations of the trend lines fitted to the plots of tendon excursion against joint angle of flexion in *Haf* (*Hylobates lar*)

Muscle tendon unit	Equation	R^2
Gluteus maximus at hip	$y = -0.23x^3 + 0.80x^2 - 1.26x + 1.73$	0.82
Adductor magnus at hip	$y = 0.50x^3 - 2.74x^2 + 3.26x + 0.64$	0.97
Semitendinosus at hip	$y = -0.75x^2 + 0.51x + 4.31$	0.70
Semimembranosus at hip	$y = -0.75x^2 + 0.51x + 4.31$	0.70
Rectus femoris at hip	$y = -1.15x - 0.52$	0.83
Long head of biceps femoris at hip	$y = 0.84x^3 - 4.08x^2 - 0.12x + 12.34$	0.96
Gracilis at hip	$y = 3.81x^2 - 10.33x + 7.46$	0.94
Long head of biceps femoris at knee	$y = -0.13x^2 + 0.75x - 0.03$	0.96
Short head of biceps femoris at knee	$y = -0.81x + 2.69$	0.84
Semitendinosus at knee	$y = 0.25x^2 + 2.65x - 1.42$	1.00
Semimembranosus at knee	$y = 0.05x^2 + 1.00x - 0.17$	0.98
Lateral vastus at knee	$y = 0.09x^3 - 0.49x^2 + 0.25x + 1.08$	0.95
Gracilis at knee	$y = 0.25x^2 + 2.65x - 1.42$	1.00
Lateral gastrocnemius at knee	$y = -0.03x^2 + 0.34x + 0.33$	0.92
Triceps surae at ankle	$y = -0.40x^2 - 0.38x + 5.34$	0.97
Flexor tibialis at ankle	$y = -0.13x^2 + 0.04x + 0.71$	0.83
Tibialis anterior at ankle	$y = -0.04x^2 + 0.64x - 0.07$	0.96
Tibialis posterior at ankle	$y = 0.11x^2 - 0.95x + 1.68$	1.00
Extensor digitorum longus at ankle	$y = 0.20x^2 + 0.53x - 0.24$	0.97

occurred in full extension. The moment arm of m gastrocnemius medialis at the knee was always linear and also either decreased (*Pp*, *Gj*, *Oam* and *Ojm*) or remained constant (*Gp*, *Gm*, *Ojf* I, *Ojf* II and *Pt*) with joint flexion. Maximum moment arms occurred in full extension.

Moment arms of muscles crossing the ankle joint

The moment arm of m. triceps surae at the ankle was remarkably similar in all subjects, being linear in shape and increasing with increasing joint dorsiflexion. However, moment arms were relatively longer at the end range of dorsiflexion in *Gp* and *Gm*. Maximum moment arms occurred in full dorsiflexion. The moment arm of m. flexor tibialis at the ankle was also similar in all subjects but it was always relatively shorter than that of m. triceps surae. Its moment arm was also linear in shape, increasing (*Pp*, *Gp*, *Oam*, and *Haf*) or remaining constant (*Gj*, *Gm*, *Ojm* and *Ojf*) with joint dorsiflexion. It was relatively long in *Gp* (a maximum of 17% of tibia length) when compared with the other subjects (maximum moment arms ranged from 3 to 10% of tibia length) and maximum moment arms occurred in full dorsiflexion. The moment arm of m. flexor fibularis at the ankle was either parabolic or linear in shape,

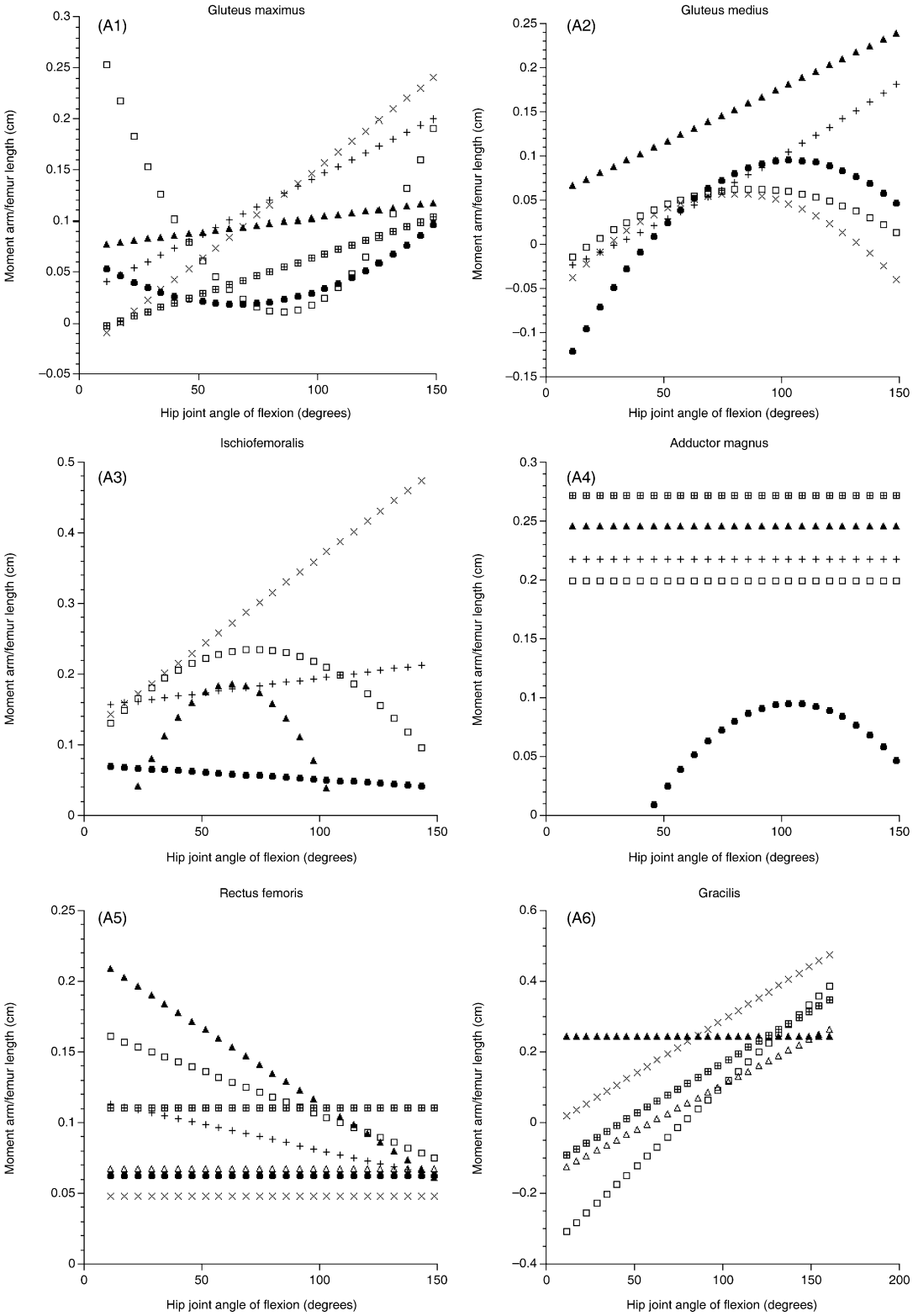

Fig. 2 Variation in muscle moment arm length about the (A) hip, (B) knee and (C) ankle joints. Open square (*Pp*), closed square (*Gp*), open triangle (*Gj*), X (*Gm*), closed triangle (*Oam*), cross (*Ojm*), open circle (*Ojf*), closed circle (*Haf*), hatched square (*Pt*). Zero degrees represents full hip extension (pelvis and femur aligned), knee extension (femur and tibia aligned) and ankle plantar flexion (tibia and foot aligned). Moment arms have been normalized by dividing by either femur length (hip and knee joint) or tibia length (ankle). Subject name abbreviations are provided in Table 1. There were two heads of gastrocnemius medialis (I & II) in *Ojf* (see Results). *Pt* data were taken directly from Thorpe et al. (1999). Gluteus maximus at hip for *Pt* is our own unpublished data.

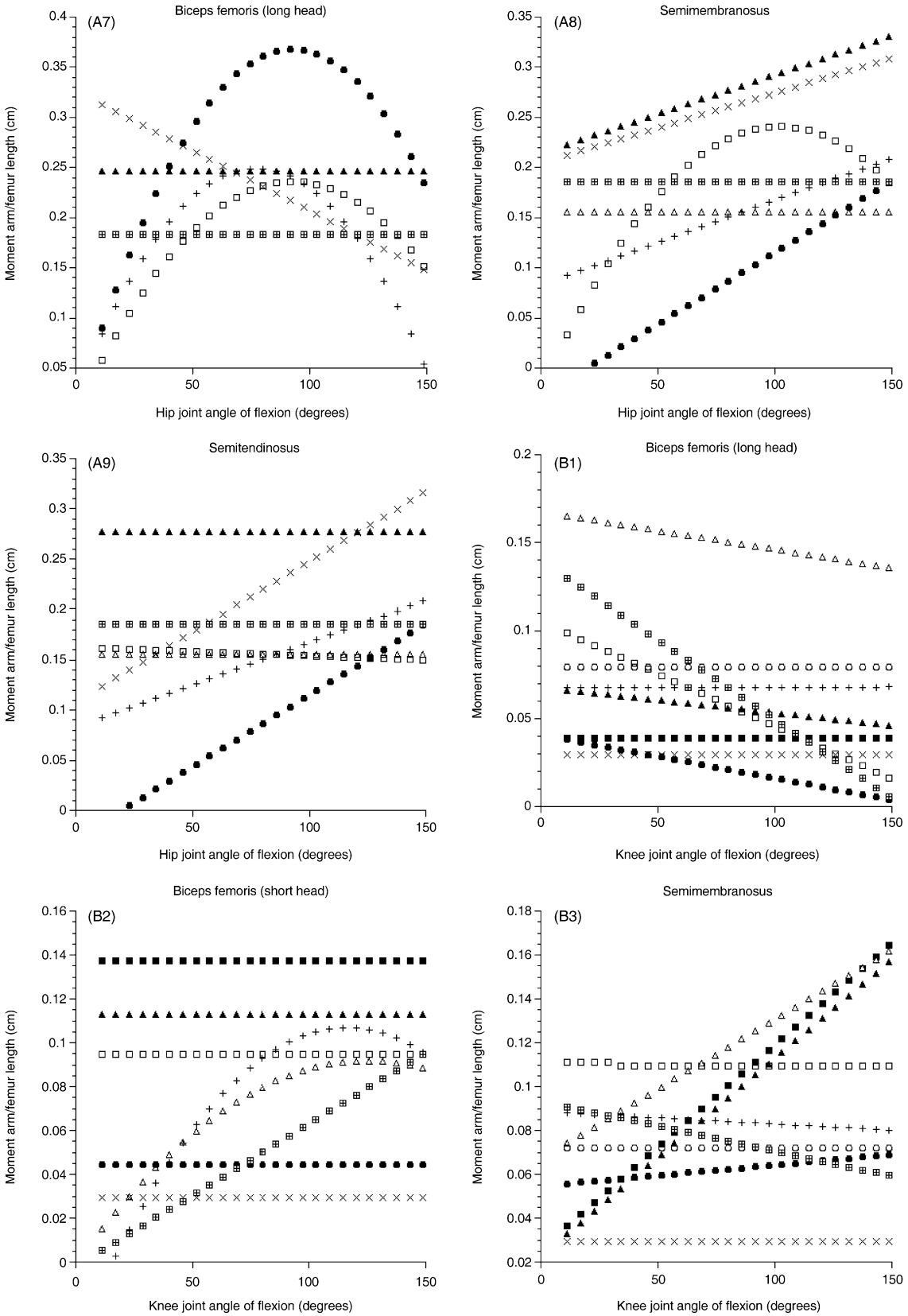

Fig. 2 *Continued*

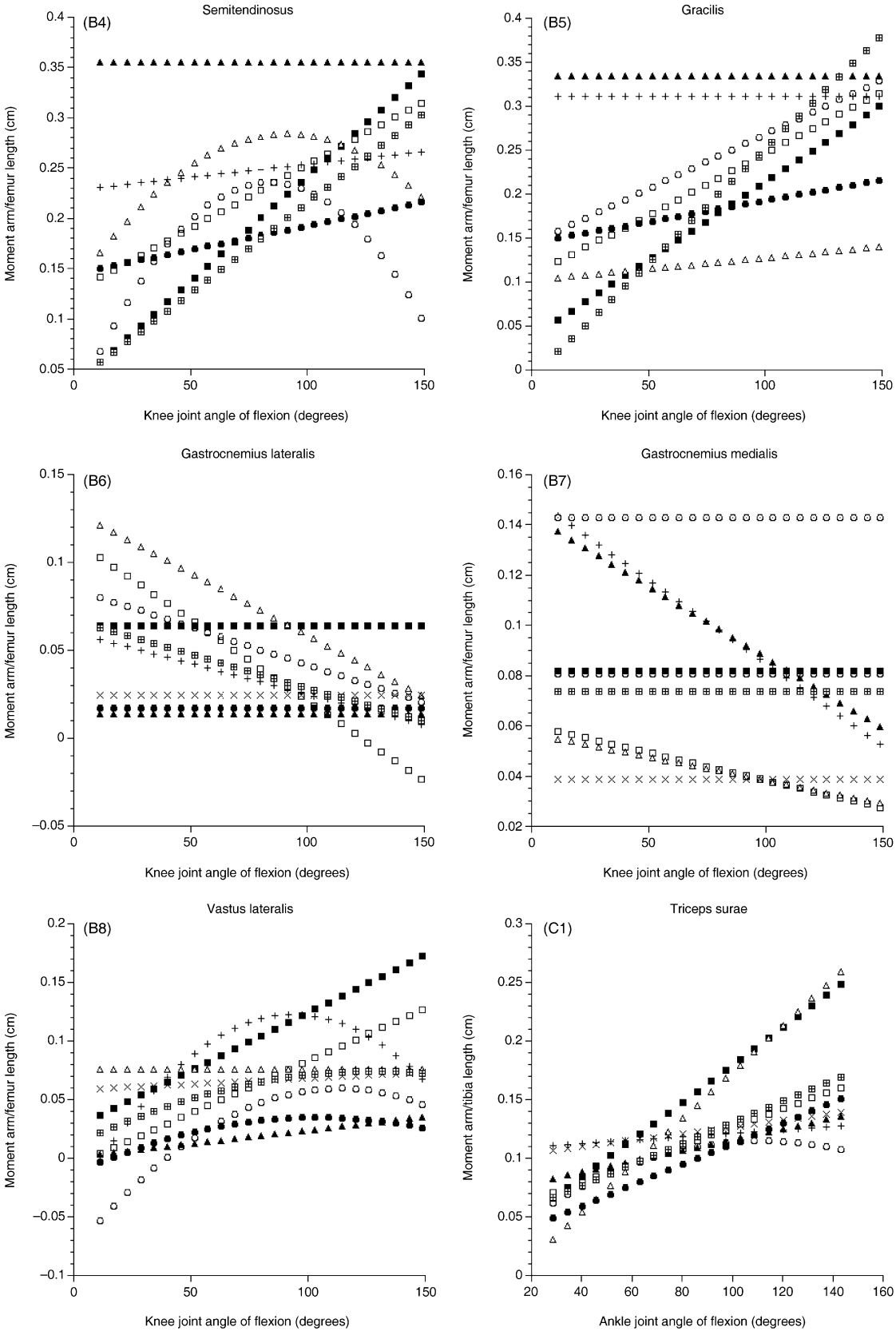

Fig. 2 *Continued*

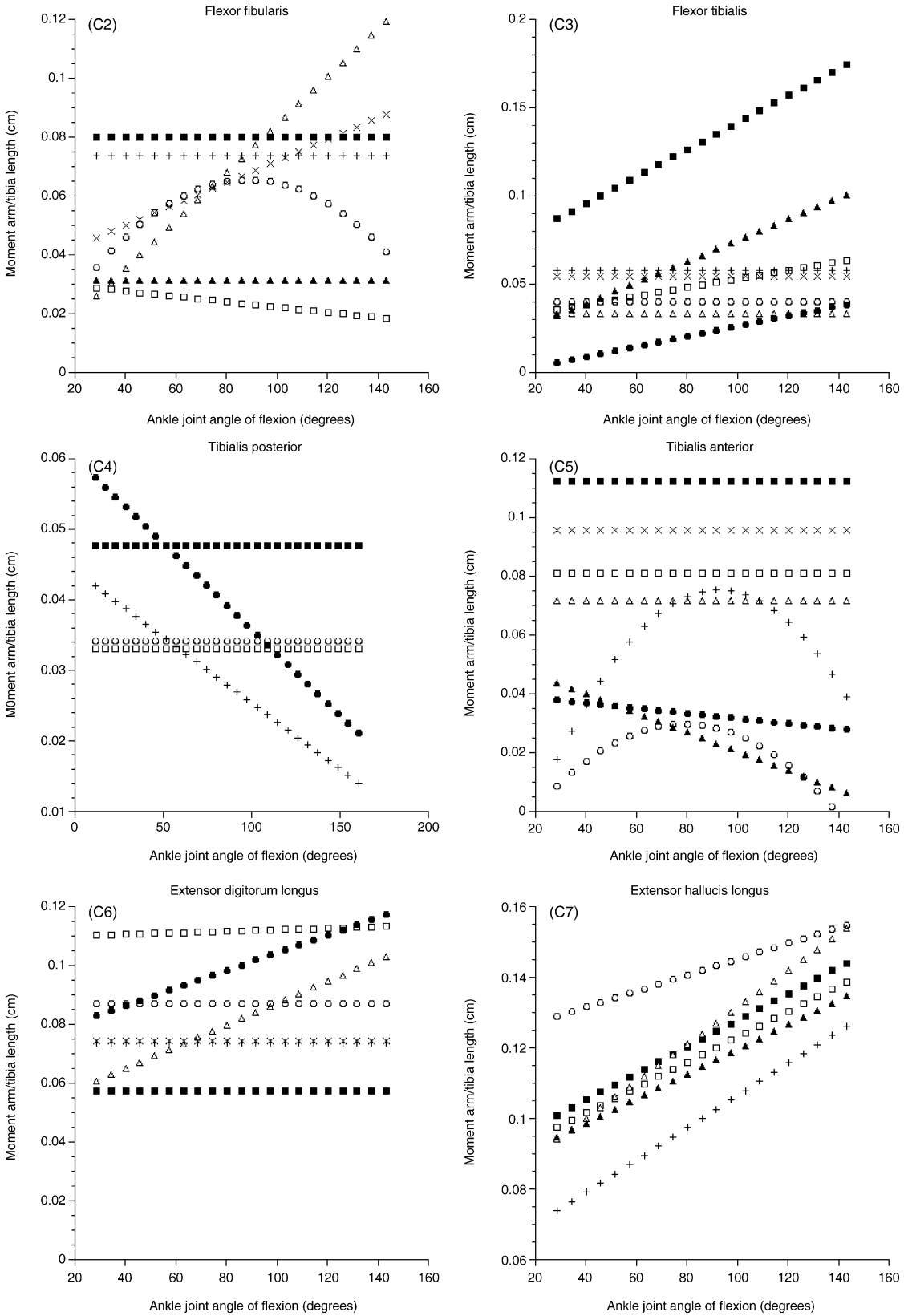

Fig. 2 *Continued*

Table 3 Maximum muscle moment arm as a percentage of either femur (hip and knee) or tibia (ankle) length

Muscle	*Pp*	*Gp*	*Gj*	*Gm*	*Oam*	*Ojm*	*Ojf*	*Haf*	*Pt*†	*Hs*
Gluteus maximus at hip	19	–	–	24	12	20	–	10	10	
Gluteus medius at hip	1	–	–	6	24	18	–	5	–	
Ischiofemoralis at hip	23	–	–	47	19	21	–	7	–	
Long head of biceps femoris at hip	24	–	–	30	25	25	–	37	18	25‡/16¶
Semitendinosus at hip	16	–	16	32	28	21	–	19	19	
Semimembranosus at hip	24	–	16	31	33	21	–	19	19	
Gracilis at hip	39	–	27	48	26	–	–	–	35	
Adductor magnus at hip	26	–	–	–	25	22	–	10	27	
Rectus femoris at hip	15	–	7	5	20	11	–	6	11	10‡/7¶
Long head of biceps femoris at knee	10	4	17	3	7	7	8	4	13	3‡/8§/7¶
Short head of biceps femoris at knee	9	14	9	3	11	11	–	4	9	
Semitendinosus at knee	31	34	28	–	36	27	24	22	30	23§
Semimembranosus at knee	11	16	16	3	16	9	7	7	9	8§
Gracilis at knee	32	30	14	–	33	31	33	22	38	
Vastus lateralis at knee	13	17	8	7	4	12	6	3	7	14‡/13§/10¶
Gastrocnemius medialis at knee	6	8	5	4	14	14	8	–	7	5‡/5¶
Gastrocnemius medialis II* at knee	–	–	–	–	–	–	14	–	–	
Gastrocnemius lateralis at knee	10	6	12	2	1	6	8	2	6	
Triceps surae at ankle	16	25	26	14	14	13	11	15	17	11¶
Flexor tibialis at ankle	6	17	3	5	10	6	4	4	–	
Flexor fibularis at ankle	3	8	12	9	3	7	7	–	–	
Tibialis anterior at ankle	9	11	7	10	4	8	3	4	–	
Tibialis posterior	3	5	–	–	–	4	3	5	–	
Extensor digitorum longus at ankle	11	6	10	7	–	7	9	12	–	
Extensor hallucis longus at ankle	14	14	15	–	13	13	15	–	–	

*Gastrocnemius medialis had two heads in *Ojf*, see Results.
†*Pt* data were taken directly from Thorpe et al. (1999).
Hs data were taken from ‡Visser et al. (1990), §Herzog & Read (1993) and ¶Thorpe et al. (1999). Raw moment arm data from Herzog & Read (1993) were divided by a hypothetical femur length of 40 cm (as published in Visser et al. 1990) in order to determine moment arm length as a percentage of femur length.

increasing then decreasing (*Ojf*), just increasing (*Gj* and *Gm*), just decreasing (*Pp*) or remaining constant (*Gp*, *Oam* and *Ojm*) with joint dorisflexion. The moment arm of m. tibialis anterior at the ankle varied widely between the subjects. It was parabolic or linear in shape, increasing then decreasing (*Ojm* and *Ojf*), just decreasing (*Oam and Haf*) or remaining constant (*Pp*, *Gp*, Gj and Gm) with joint dorsiflexion. It was relatively short throughout joint motion in *Oam*, *Ojf* and *Haf*. Maximum moment arms occurred either in the mid range of joint motion or in full extension. The moment arm of m. tibialis posterior at the ankle was always linear in shape, decreasing (*Ojm* and *Haf*) or remaining constant (*Pp*, *Gp* and *Ojf*) with joint dorsiflexion. Maximum moment arms occurred in full plantarflexion. The moment arm of m. extensor hallucis longus at the ankle was linear in shape and remarkably similar between subjects (*Pp*, *Gp*, *Gj*, *Oam*, *Ojm* and *Ojf*), increasing with joint dorsiflexion. Maximum moment arms occurred in full dorsiflexion. The moment arm of m. extensor digitorum longus at the ankle was also linear and similar between subjects, increasing (*Gm* and *Haf*) or remaining constant (*Pp*, *Gp*, *Gj*, *Ojm* and *Ojf*) with joint dorsiflexion. Maximum moment arms occurred in full dorsiflexion.

Discussion

Muscles generate forces which cause the rotation of adjacent limb segments about joints. The rotational force or moment about a joint is determined not only by the physiological cross-sectional area (PCSA) and maximum isometric stress of a muscle, but also by muscle moment arms, which can vary according to joint posture. Many of the muscles studied had moment arms that varied through the joint range of motion. Such variation in moment arm is advantageous in that it enables muscles to function differently at different joint or limb postures. In spite of this, most biomechanical studies that use moment arms to estimate muscle

moments treat moment arms as constant values. Few have directly considered how muscle moment arms depend on joint posture. This is to a great extent because reliable comparative interpretation of the significance of dynamic moment arm data is difficult outside of a full three-dimensional multibody dynamic analysis. Such studies are outside the scope of this paper. However, provision of moment arm curves permits dynamic analyses to be carried out, if inertial models, kinematics and ground reaction forces are also available.

In general, the present data, when compared with those for humans (Leardini & O'Connor, 2002; Krevolin et al. 2004) and horses (Brown et al. 2003), indicated that non-human apes appear to have muscles that are well suited for moving joints through large ranges, extending the finding of Thorpe et al. (1999) for chimpanzees.

Variation in moment arms

The shape and magnitude of moment arm curves varied both within and between subjects, species and muscle groups. However, at least some of the variation observed here may also be attributed to experimental techniques and or/scaling methods, the details of which will be addressed later in this discussion.

Muscles crossing the hip joint

At the hip joint, the general trend was for long moment arms (maximum moment arms were often in excess of 30% of femur length); these moment arms tended to increase with increasing flexion. In some muscles, moment arms would then decrease towards the end ranges of flexion. Maximum moment arms therefore occurred either in the mid range of joint motion or at maximum joint flexion. The exception to this was the moment arm of m. gluteus medius in *Pp* and *Haf* (which decreased then increased with joint flexion) and m. rectus femoris in *Pp*, *Oam* and *Ojm* (which decreased with joint flexion). That maximum muscle torques should be generally achieved in flexed postures seems consistent with the fact that most great apes (excluding orang-utans, see Thorpe & Crompton, 2004) maintain flexed hip postures during the propulsive phase of both terrestrial quadrupedal and arboreal vertical climbing gaits (Isler, 2005). Hip joint moment arms were often relatively small in *Haf* (specifically: m. gluteus maximus, m. semitendinosus, m. semimembranosus and m. rectus femoris). This may indicate a difference in hip joint function in the gibbon. Indeed, with a maximum moment arm of 37% of femur length, m. biceps femoris looks to be the major hip extensor in the gibbon, particularly in the mid range of joint motion. In other non-human apes, m. biceps femoris, m. semimembranosus and m. semitendinosus had similarly large moment arms.

Muscles crossing the knee joint

There was a greater amount of intersubject variation in the moment arms of muscles crossing the knee joint. In general, as for the hip, moment arms increased with joint flexion. However, many remained constant and some were parabolic, decreasing again towards the end range of flexion. Furthermore, in some subjects, the moment arm of m. biceps femoris, m. gastrocnemius lateralis and m. gastrocnemius medialis actually decreased with joint flexion. M. biceps femoris is said to be a knee joint flexor, although it inserts very close to the joint centre. Its moment arm was greatest in extension and thus it may be important in initiating flexion or in supporting the flexed knee joint during the stance phase.

Muscles crossing the ankle joint

Moment arms of muscles crossing the ankle joint were remarkably similar both within and between subjects for m. triceps surae, m. flexor tibialis, m. extensor digitorum longus and m. extensor hallucis longus. Uniformity in the moment arms of muscles crossing the ankle joint is perhaps not surprising as there is less scope for variation in muscle line of action compared with say muscles crossing either the hip joint or the knee joint. The other muscles (m. flexor fibularis, m. tibialis anterior and m. tibialis posterior) were more variable in their moment arms and this may at least partly be due to the fact that they cross the lateral aspect of the joint. In such cases, variation in moment arms may also depend on how well the joint is fixed in purely sagittal plane motion.

Comparison of human and non-human ape moment arms

Data on human hindlimb muscle moment arms have been published previously. However, there is no single study providing data on all of the muscles studied here.

In order to compare non-human ape muscle moment arms with those of humans, data were selected from comparable papers (Visser et al. 1990; Herzog & Read, 1993; Thorpe et al. 1999) and are provided in Table 3 as a percentage of femur length. Human hindlimb (maximum) muscle moment arms were similar (yet at the lower end of the range) to those observed in the non-human apes. This is perhaps not surprising as hindlimb geometry is based on the same basic pattern and muscles inserted onto similar areas of the bones.

Architecture, geometry and functional capacity

It is well known that muscle architecture is intimately related to muscle function. The functional capacity of a muscle is, however, not only dictated by the number and arrangement of its fascicles but also by its moment arm. The important ratio is muscle fascicle length/moment arm length; a high MFL : MAL ratio indicates the ability to move a joint through large ranges (Alexander et al. 1981; Alexander, 1993). Thorpe et al. (1999) compared this ratio for hindlimb functional muscle groups in the common chimpanzee and humans and observed that common chimpanzee hindlimb muscles had higher MFL : MAL ratios (and thus presumably a greater capacity to generate force over a wide range of motion) than human hindlimb muscles. They attributed this difference to differences in hindlimb function, i.e. the greater part of human bipedal locomotion requires force generation over a rather limited range whereas chimpanzees continually use their limbs in a wide variety of postures. Our calculations also suggest that non-human ape hindlimb muscles are better designed for moving joints through wide ranges. The difference, however, was not as marked as in the chimpanzee–human comparison (Table 4). This is at least partly because we used maximum moment arm in our calculations rather than moment arm at the mid point of a bipedal stride (which posture was of particular relevance to the paper by Thorpe et al. 1999). *Pp* and *Pt* had remarkably similar MFL : MAL ratios for all muscles except quadriceps at knee, which was twice as large in *Pt*. This was because the maximum moment arm of m. vastus lateralis was 13% of femur length in *Pp* but only 7% of femur length in *Pt*. Thorpe et al. measured the moment arm of rectus femoris and vastus lateralis at the knee together, which might explain this difference. In the gorillas and orang-utans, proximal limb muscle MFL : MAL ratios varied somewhat within species but distal limb muscle MFL : MAL ratios were relatively similar. The orang-utans had relatively large MFL : MAL ratios for the deep pedal flexor and dorsiflexor muscles. The juvenile orang-utans also had large MFL : MAL ratios for triceps at ankle. This is because the orang-utans had long fascicles in the distal limb muscles compared with the other subjects (Payne et al. 2006). Orang-utans are described as being quadrumanous as they use their feet as a second pair of hands. The foot is used in numerous different positions during locomotion (i.e. in both tension and compression) and, as such, muscles with high MFL : MAL ratios would be particularly useful. The gibbon had large MFL : MAL ratios for most proximal limb muscles (gluteals, adductors, quadriceps at knee and triceps at knee) and this was due to relatively short moment arms (in spite of having relatively short muscle fascicles). Thus, gibbon proximal hindlimb muscles are well designed for achieving large ranges of joint motion (Hildebrand, 1995). Gibbons are

Table 4 Ratio of mean muscle fascicle length/mean maximum muscle moment arm

	Hs	*Pt*	*Pp*	*Gp*	*Gj*	*Gm*	*Oam*	*Ojm*	*Ojf*	*Haf*
Gluteals	–	3.03	2.39	–	–	1.26	1.42	1.62	–	4.09
Hamstrings (hip)	1.3	3.72	3.16	–	4.88	1.91	1.18	3.12	–	1.97
Adductors	5.3	2.34	2.23	–	2.34	0.95	2.32	3.34	–	4.87
Hip flexors	1.1	2.46	2.02	–	4.91	3.52	1.50	3.68	–	3.33
Quadriceps (knee)	1.4	4.41	2.29	2.23	4.93	7.09	8.00	3.42	3.12	5.52
Hamstrings (knee)	2.8	2.10	2.38	2.33	3.04	–	1.47	3.42	2.36	2.23
Triceps (knee)	2.1	4.07	4.19	4.55	2.96	7.16	3.52	4.36	3.32	8.79
Triceps (ankle)	0.5	1.61	1.72	1.26	0.91	1.39	1.56	3.70	3.34	1.09
Pedal digital flexors	–	–	6.58	3.61	3.17	2.56	6.23	6.65	7.78	3.60
Dorsiflexors	–	–	3.01	3.24	2.57	1.81	5.31	4.89	4.75	2.22

Fascicle lengths for each functional muscle group were calculated as a weighted harmonic mean (Payne et al. 2006). Moment group arms are the mean of the maxima of the muscles in that group.

specialists in ricochetal brachiation, a mode of locomotion that, once initiated, requires very little new energy to maintain. However, when atop branches or on the ground, gibbons employ a bipedal running gait. With this in mind, one might have expected gibbons to have hindlimb muscles capable of generating large torques. That this is not the case indicates that gibbon and human running is mechanically different. In our previous paper (Payne et al. 2006) gibbons were found to have relatively long tendons compared with the other non-human apes. This difference was attributed to either weight reduction or elastic recoil needed for running and jumping.

Experimental procedure

The tendon travel technique has been used to measure moment arms in many different species. However, many of the data pertain to distal limb muscles. This may be because distal limb muscles have long cord-like tendons with approximately circular joint paths, thus lending themselves to the experimental procedure. In this study, we attempted to determine the moment arms of as many of the major hindlimb muscles as possible, including large-volume, fan-shaped muscles of the proximal limb (see below). Comparison of data was always going to be difficult as our sample comprised only nine cadavers, including five species of ape (two of which were juveniles). In addition, many of the hip joint muscles were rendered useless during limb removal (prior to our obtaining the specimens). Finally, data could only be processed and checked long after the muscles had been discarded. In spite of the above, we have succeeded in collecting a large volume of valuable data on the architecture and geometry of hindlimb muscles in apes. However, these practical difficulties should be considered when addressing unexpected variation in moment arm data, both within and between the species studied here.

We observed a large amount of variation within individual moment arm curves. However, the shape of the moment arm curve was not always the same in members of the same species. For example, in semimembranosus at the hip (see Fig. 2), several subjects showed no change in moment arm length (*Gj*) whereas in others it ranged by up to 30% of femur length (*Gm*). Variation in the shape and magnitude of the moment arm curve of the same muscle in the same species could be related to conformational differences (i.e. differences in skeletal shape and form) or alternatively/additionally to practical difficulties associated with using the tendon travel technique. For example, there is a large coronal plane component to much of great ape hindlimb motion which we were not able to address here. In all subjects, the hip joint was capable of a greater range of flexion/extension when attempted with concomitant abduction (which is probably closer to hip motion *in vivo*), yet limb motion was of necessity restricted to the sagittal plane as this was the plane of the photographic images from which length and angle measurements were obtained. An alternative approach would be to measure length change using a potentiometer attached to the end of the string but this would not be practical in muscles with wide areas of origin and/or insertion (i.e. fan-shaped muscles, see Materials and methods). This is because, in larger proximal limb muscles such as m. gluteus maximus, tendon travel is measured as the distance between pins that have been inserted into the mid point of the origin and insertion of the muscle. Furthermore, if the muscle line of action deviates from the sagittal plane (i.e. the plane of the camera), changes in MTU length (i.e. tendon travel) cannot be measured accurately from the resulting images. In spite of this, the moment arm curves obtained for fan-shaped muscles apearred to be reasonable (i.e. maximum moment arm length ranged from 1 to 24% of femur length in m. gluteus maximus and m. gluteus medius) and compared well with those obtained for other hip joint muscles (e.g. semimembranosus at hip in which maximum moment arm lengths ranged from 19 to 33% of femur length). Greater accuracy of measurement may have been achieved by collecting tendon travel data at a larger number of joint positions. The sensitivity of the tendon travel technique to the number of measurements taken during each cycle of joint motion should be tested before further use of the technique.

Scaling

The ontogenetic scaling of moment arms has not yet been investigated. However, in order to compare moment arms among subjects of varying species, age and size, we scaled moment arms by femur/tibia length. We used segment lengths to scale data because body mass data were not available for all subjects. It may of course be that some of the inter- and intraspecific differences observed here are related to scaling error. Ideally,

variation in moment arms both within- and between-species should be tested in a series of controlled experiments involving larger numbers of subjects that have been matched for sex, age and body mass. Such a data set would, however, be difficult to acquire in apes as fresh-frozen ape cadavers are extremely scarce.

Conclusions

Ape hindlimb muscle moment arms varied considerably through the joint range of motion. Proximal limb moment arms varied more than distal limb moment arms. The shape of the moment arm curves varied between muscles and between the same muscle in different/the same species. However, maximum moment arm length and range in moment arm length as a percentage of either femur or tibia length was similar in the apes studied here.

Acknowledgements

We would like to thank the North of England Zoological Society, Bristol Zoo, Zoo Basel, Zoo Zurich and Knie's Kinderzoo Rapperswil for provision of ape cadavers. Individuals who helped greatly in this regard include Mr Nicholas Ellerton (then N.E.Z.S.), at the University of Liverpool: Ray Burniston; at the Institute of Anthropology, Zurich: Bob Martin, Beno Schoh and Marcus Gisi. Daniel Oppliger, Basel, also gave invaluable assistance. This research was funded by the Natural Environment Research Council, the Biotechnology and Biological Sciences Research Council, the Engineering and Physics Research Council, the Royal Society, the L.S.B. Leakey Foundation, the Leverhulme Trust, the University of Liverpool and the Adolph Schultz Foundation, Zurich.

References

Alexander RM, Jayes AS, Maloiy GMO, Wathuta EM (1981) Allometry of the leg muscles of mammals. *J Zool Lond Series A* **194**, 227–267.

Alexander RM (1993) Optimization of structure and movement of the legs of animals. *J Biomech* **26** (Suppl. 1), 1–6.

An KN, Hui FC, Morrey BF, Linscheid RL, Chao EY (1981) Muscles across the elbow joint: a biomechanical analysis. *J Biomech Eng* **14**, 659–669.

An KN, Takahashi K, Harrigan TP, Chao EY (1984) Determination of muscle orientations and moment arms. *J Biomech Eng* **106**, 280–282.

Arnold AS, Salinas S, Asakawa DJ, Delp SL (2000) Accuracy of muscle moment arms estimated from MRI-based musculoskeletal models of the lower extremity. *Computer Aided Surg* **5**, 108–119.

van den Bogert AJ, Schamhardt HC, Crowe A (1989) Simulation of quadrupedal locomotion using a rigid body model. *J Biomech* **22**, 33–41.

Brown N, Pandy M, Kawcak C, McIlwraith W (2003) Moment arms about the carpal and metacarpophalangeal joints for flexor and extensor muscles in the equine forelimb. *Am J Vet Res* **64**, 351–357.

Carrano MT, Hutchinson JR (2002) Pelvic and hindlimb musculature of *Tyrannosaurus rex* (Dinosauria: Theropoda). *J Morph* **253**, 207–228.

Crompton RH, Yu L, Weijie W, Gunther MG, Savage R (1998) The mechanical effectiveness of erect and 'bent-hip, bent-knee' bipedal walking in *Australopithecus afarensis*. *J Hum Evol* **35**, 55–74.

Graichen H, Englemeier KH, Reiser M, Eekstein F (2001) An in vivo technique for determining 3D muscular moment arms in different joint positions and during muscular activation – application to the supraspinatus. *Clin Biomech* **16**, 389–394.

Herzog W, Read LJ (1993) Lines of action and moment arms of the major force-carrying structures crossing the human knee joint. *J Anat* **182**, 213–230.

Hildebrand M (1995) *Analysis of Vertebrate Structure*. New York: John Wiley & Sons, Inc.

Hughes R, Nieber G, Liu J, An K (1998) Comparison of two methods for computing abduction moment arms of the rotator cuff. *J Biomech* **31**, 157–160.

Hutchinson JR (2002) The evolution of hindlimb tendons and muscles on the line to crown-group birds. *Comp Biochem Physiol A Mol Integr Physiol* **133**, 1051–1086.

Hutchinson JR, Garcia M (2002) *Tyrannosaurus* was not a fast runner. *Nature* **415**, 1018–1021 (Erratum. **416**, 349).

Hutchinson JR (2004) Biomechanical modeling and sensitivity analysis of bipedal running ability. II. Extinct taxa. *J Morph* **262**, 441–461.

Isler K (2005) 3D-kinematics of vertical climbing in hominoids. *Am J Phys Anthropol* **126**, 66–81.

Juul-Kristensen B, Bojsen-Moller F, Holst E, Ekdahl C (2000) Comparison of muscle sizes and moment arms of two rotator cuff muscles measured by ultrasonography and magnetic resonance imaging. *Eur J Ultrasound* **11**, 161–173.

Krevolin JL, Pandy MG, Pearce JC (2004) Moment arm of the patellar tendon in the human knee. *J Biomech* **37**, 785–788.

Landsmeer JM (1961) Studies in the anatomy of articulation. II. Patterns of movement of bi-muscular, bi-articular systems. *Acta Morph Neerl Scand* **3**, 304–321.

Leardini A, O'Connor JJ (2002) A model for lever-arm length calculation of the flexor and extensor muscles at the ankle. *Gait Posture* **15**, 220–229.

Li Y, Crompton RH, Gunther M, Wang W, Savage R (2002) Reconstructing the mechanics of quadrupedalism in an extinct hominoid. *Z Morph Anthropol* **83**, 265–274.

Lieber RL, Boakes JL (1988a) Muscle force and moment arm contributions to torque production in frog hindlimb. *Am J Physiol* **254**, C769–C772.

Lieber RL, Boakes JL (1988b) Sarcomere length and joint kinematics during torque production in frog hindlimb. *Am J Physiol* **254**, C759–C768.

Lieber RL, Friden J (2001) Clinical significance of skeletal muscle architecture. *Clin Orthop Rel Res* **383**, 140–151.

Maganaris CN (2004) A predictive model of moment-angle characteristics in human skeletal muscle: application and validation in muscles across the ankle joint. *J Theor Biol* **230**, 89–98.

Marzke MW, Longhill JM, Rasmussen SA (1988) Gluteus maximus muscle function and the origin of hominid bipedality. *Am J Phys Anthropol* **77**, 519–528.

Meershoek LS, van den Bogert AL, Schamhardt HC (2001) Model formulation and determination of in vitro parameters of a noninvasive method to calculate flexor tendon forces in the equine forelimb. *Am J Vet Res* **62**, 1585–1593.

Nagano A, Umberger BR, Marzke MW, Gerritsen KGM (2005) Neuromusculoskeletal computer modeling and simulation of upright, straight-legged, bipedal locomotion of *Australopithecus afarensis* (A.L. 288–1). *Am J Phys Anthropol* **126**, 2–13.

Nemeth G, Ohlsen H (1985) *In vivo* moment arm lengths for hip extensor muscles at different angles of hip flexion. *J Biomech* **18**, 129–140.

Payne RC, Crompton RH, Isler K, et al. (2006) Morphological analysis of the hindlimb in apes and humans. I. Comparative anatomy. *J Anat* **208**, 709–724.

Pontzer H, Wrangham RW (2004) Climbing and the daily energetic cost of locomotion in wild chimpanzees: implications for hominoid locomotor evolution. *J Hum Evol* **46**, 317–335.

Sellers WI, Cain GM, Wang W-J, Crompton RH (2005) Stride lengths, speed and energy costs in walking of *Australopithecus afarensis*: using evolutionary robotics to predict locomotion of early human ancestors. *J R Soc Interface* **5**, 431–441.

Sellers WI, Dennis LA, Crompton RH (2003) Predicting the metabolic energy costs of bipedalism using evolutionary robotics. *J Exp Biol* **206**, 1127–1136.

Sellers WI, Dennis LA, Wang W-J, Crompton RH (2004) Evaluating alternative gait strategies using evolutionary robotics. *J Anat* **204**, 343–351.

Spoor CW, van Leeuwen JL (1992) Knee muscle moment arms from MRI and from tendon travel. *J Biomech* **25**, 201–206.

Thorpe SKS, Crompton RH, Günther MM, Ker RF, Alexander RM (1999) Dimensions and moment arms of the hind- and forelimb muscles of common chimpanzees (*Pan troglodytes*) *Am J Phys Anthropol* **110**, 179–199.

Thorpe SKS, Crompton RH (2004) Locomotor ecology of wild orang-utans (*Pongo pygmaeus abelii*) in the Gunung Leuser ecosystem, Sumatra, Indonesia: a multivariate analysis using log-linear modelling. *Am J Phys Anthropol* **127**, 58–78.

Visser JJ, Hoogkamer JE, Bobbert MF, Huijing PA (1990) Length and moment arm of human leg muscles as a function of knee and hip-joint angles. *Eur J Appl Physiol* **61**, 453–460.

Wang WJ, Crompton RH (2004a) Analysis of the human and ape foot during bipedal standing with implications for the evolution of the foot. *J Biomech* **12**, 1831–1836.

Wang WJ, Crompton RH (2004b) The role of load-carrying in the evolution of modern body proportions. *J Anat* **204**, 417–430.

Wang WJ, Crompton RH, Li Y, Gunther MM (2003) Energy transformation during erect and bent-hip-bent-knee walking by humans with implications for the evolution of bipedalism. *J Hum Evol* **44**, 563–580.

Wang W, Crompton RH, Carey TS, et al. (2004) Comparison of inverse-dynamics musculo-skeletal models of AL 288-1 *Australopithecus afarensis* and KNM-WT 15000 *Homo ergaster* to modern humans, with implications for the evolution of bipedalism. *J Hum Evol* **47**, 453–478.

Wilson AM, McGuigan MP, Su A, Van den Bogert AJ (2001) Horses damp the spring in their step. *Nature* **414**, 895–898.

Wilson AM, Watson JC, Lichtwark GA (2003) A catapult mechanism for rapid limb protraction. *Nature* **421**, 35–36.

Zajac FE (1992) How muscle-tendon architecture and joint geometry affect the capacity of muscles to move and exert force on objects: a review with application to arm and forearm tendon transfer design. *J Hand Surg* **17A**, 799–804.